Cadernos Lab. Xeolóxico de Laxe
Coruña. 2001. Vol. 26, pp. 179-190

ISSN: 0213-4497

Geostatistical interpolation of topographical field data in order to obtain a DEM of a small forest catchment in Northwest Spain

Interpolación geoestadística de datos topográficos para obtener un MED de una pequeña cuenca forestal en el noroeste de España

THONON, I.[1] & CACHEIRO POSE, M.[2]

ABSTRACT

This article gives an example of the elaboration of a digital elevation model (DEM) with the aid of geostatistics, using the case of a small experimental catchment near Arcos de la Condesa in Galicia, Spain. A DEM is a necessary tool in present-day erosion and landscape modelling. The geostatistical method of DEM construction involves six steps, starting with the removal of the drift and ending with the final interpolation. The drift was almost completely eliminated by a first order trend surface. After it had been confirmed that no heteroscedacity is present in the data set, the resulting experimental variogram was fitted by an anisotropic Gaussian variogram model, which is the variogram model that is generally used for DEM interpolation. Cross validation was used to determine the optimal number of data points to be used in interpolation. The interpolation results were found to be satisfactory and the interpolation standard deviations are below the data set standard deviation. It is yet noted that this uncertainty in the DEM – although small – may influence its derivatives and subsequent model results. However, when

Cadernos Lab. Xeolóxico de Laxe
Coruña. 2001. Vol. 26, pp. 179-190

compared to other methods of DEM elaboration, the method as used here is an easy, adequate and relatively fast method, that has the major advantage of providing interpolation errors, enabling an evaluation of the interpolation result.

Key words: geostatistics, kriging, interpolation, anisotropy, DEM, GIS.

(1) Department of Physical Geography, Faculty of Geographical Sciences, Utrecht University, PO Box 80.115, 3508 TC, Utrecht, The Netherlands.
(2) Department of Soil Sciences, Faculty of Sciences, University of A Coruña, A Zapateira, 15.071, A Coruña, Spain.

INTRODUCTION

A DEM is a necessary tool for the calculation of slope, aspect, drainage direction and other landscape variables, which are frequently used in erosion modelling. Examples of other DEM elaborations with the aid of so-called geostatistics or kriging can be found in CACHEIRO POSE *et al.* (1999) and DAFONTE DAFONTE *et al*. (1999). In this paper, the delineation of a digital elevation model (DEM for short) on basis of geodetic measured field data is described. The catchment under consideration is about 2.5 ha and is located in the region of Galicia in the northwest of Spain.

The following assumes a basic knowledge of geostatistics. When this is not present, it is referred to general textbooks such as ISAAKS & SRIVASTAVA (1989), BURROUGH & McDONNELL (1998) or ARMSTRONG (1998) for this background.

MATERIAL AND METHODS

The data set that was used in the elaboration of the DEM consists of 307 data entries with an (arbitrary, officious) x, y and z co-ordinate. Point elevations were measured using an Abney Level geodetic instrument (Sokkia SET5A). The x and y co-ordinates are used to fix the position of the points in space, the z co-ordinates denote the height. In table 1, the descriptive statistics of the data set are given. Note that also the height has an arbitrary origin at 1000 m. It is therefore unsound to calculate the CV (coefficient of variation).

In figure 1, the histogram of the data set is given. It can be seen that the distribution appears to be about normal. This is important, because kriging (the method that is to be used for interpolation) works best with normally/Gaussian distributed data (ISAAKS & SRIVASTAVA 1989), although, strictly spoken, it is not obligatory neither a prerequisite. A normal distribution only aids in optimisation of the interpolation.

There was made use of the computer programs PCRaster (Van DEURSEN & WESSELING 1992; KARSSENBERG 1996), version 2, and Gstat (PEBESMA & WESSELING 1998; PEBESMA 1999), versions 2.0b and 2.1.0. PCRaster is a raster based GIS program, while Gstat is a geostatistical program for interpolation and simulation.

Kriging is a geostatistical method to interpolate spatially distributed point data in a sound and unbiased manner, i.e. it looks for the BLUE (best linear unbiased estimate) (ARMSTRONG 1998) using sophisticated matrix algebra and mathematical rules. This means that

n	mean	median	mode	variance	st.dev.	skewness *	kurtosis **
307	1005.13	1006.88	1008.51	46.71	6.83	-0.33	-0.24

Table 1. Basic statistics of the data set. *): skewness has an associated error of 0.14; **): kurtosis has an associated error of 0.28.

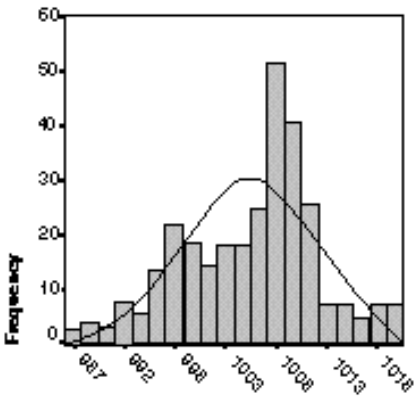

Figure 1. Distribution of the data set. Note that the distribution follows more or less a normal distribution but seems to exhibit a slight bimodality as well (as demonstrated by the presence of two peaks).

interpolation errors are minimised, because minimisation of these errors is part of the solution of the kriging system.

Kriging (named after KRIGE (1966)), i.e. the interpolation itself, is normally carried out only after the implementation of a few other basic steps:

1. checking for a trend or tendency in the data set. If a trend can be spotted (using exploratory data analysis, map analysis etc.), removal of it will improve and ease the next steps;

2. checking for heteroscedacity in the data set. Heteroscedacity means that the different sub areas of the area that is to be interpolated exhibit different amounts of variation. If this heteroscedacity is indeed present, the area has to be divided in these sub areas, because otherwise a sound interpolation cannot be guaranteed;

3. checking for anisotropy in the data set. Anisotropy means that the variograms (i.e., graphs that denote the amount of correlation between points) in the several wind directions are different from each other. Incorporating this anisotropy in the fitting of the variogram model can improve the quality of the subsequent interpolation. A check for the presence or absence of anisotropy (when absent, the data set is called to be isotropic) can be made by making a variogram map, i.e. a 3D semivariogram or semivariogram surface of the area.

4. fitting of a variogram model. When the trend is subtracted from the data set, a residual data set remains. The semivariance of these residuals is calculated and a (semi)variogram model is fitted, usually using fitting techniques as 'weighted least squares' or 'ordinary least squares';

5. cross validation. In this exercise, the models are checked on integrity and the different models that may be used can be compared to each other on basis of objective statistical measures;

6. Both, the semivariogram model and the trend surface, are used for the final interpolation of the data set. This type of kriging is called Universal or KT kriging. The trend surface is used to interpolate the global trend in the data set, the residues are interpolated by the kriging action with the variogram model.

Hereafter, the steps are explained and the results of the steps are presented and discussed.

RESULTS AND DISCUSSION

Step 1: delineation of a possible trend

The most general used trend surface is based on x and y co-ordinates. With these spatial co-ordinates, the data set values are to be predicted in the total area. This proceeds through the use of 'least squares' fitting techniques in combination with the following formula:

$$z(x, y) = b_1 \cdot x + b_2 \cdot y + b_0 \qquad \text{(Eq. 1)}$$

with: z = value (in this case height) that has to be interpolated [m]; b_n = a constant derived from the 'least squares' fitting of the trend surface through the data set; x = x co-ordinate [m]; y = y co-ordinate [m].

There also exist second, third and higher order trend surfaces. Gstat can interpolate up to a third order trend surface. The second and third one were also evaluated, but these were not used here since the first order trend surface proved to be the better one. The first order trend surface did not prove to be the best one in the sense that the surface fitted the data distribution the best (this is impossible, for a second and third order trend surface have more degrees of freedom), but the variogram that can be constructed afterwards is more sound in geostatistical sense. This will be explained later. Besides, the quality of the fit in terms of the size of the residuals of the trend surface is rather unimportant: the residuals are after all fitted by the kriging. Kriging is not influenced by the size of the residuals, only by their distribution.

In figure 2a, the fitted first order trend surface can be seen, while in figure 2b the distribution of the residuals is depicted.

Step 2: checking for heteroscedacity

In figure 2b, it can be seen that the distribution of the residuals is confined to a narrow region around 10.4 to 10.8. Because the residuals can be regarded as the unexplained variance of the trend surface, and therefore as a pseudo variance of the data set, this is a first indication that

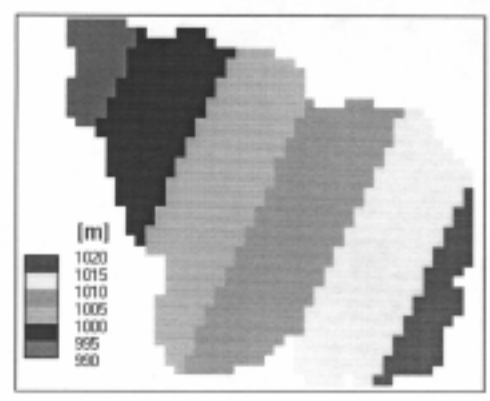

Figure 2a. The height according to the first order trend surface.

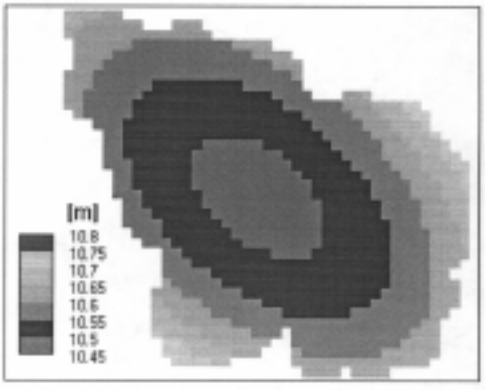

Figure 2b. The distribution of the residuals.

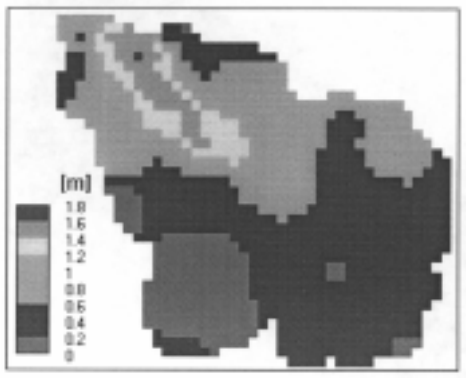

Figure 3. The standard deviation per cell as calculated for a split moving window of 30 by 30 m. Note the small differences in values and the general homogeneity of the area.

the data set probably is homoscedastic: the variance is about equally distributed over the whole area.

This is confirmed by a PCRaster model that calculates the standard deviation per split moving window: see figure 3. Note that the differences in this case are larger (the calculation method is different) but a range in standard deviation of about 2 m on a range in the data set of about 35 m is still rather small. Therefore, the data set can be considered homoscedastic. However, there does not exist an objective method to determine whether an area is homoscedastic or not; 'expert judgement' on a visual basis is the only method.

Step 3: checking for anisotropy

The check for anisotropy basically evolves in the same way as step 2: through the creation of a variogram surface and visual interpretation of this map surface. However, when it is decided that the area exhibits anisotropy, the anisotropy ratio may aid in the determination whether it is necessary or not to interpolate with an anisotropic variogram model: the closer it is to 1, the less necessary. The anisotropy ratio is calculated by dividing the range of the minor axis by the range of the major axis (see figure 4 for the explanation of these terms) in the case of geometric anisotropy. In the case of zonal anisotropy, the anisotropy ratio is the lowest sill divided by the highest sill, provided that the directions in which these sills are measured are perpendicular to each other, as in figure 4.

The variogram map is depicted in figure 5. It can be seen that the major axis is trended Northwest–Southeast (the low semivariances), directing about 140º clockwise from North. By definition, the minor axis is thus directed 50º clockwise

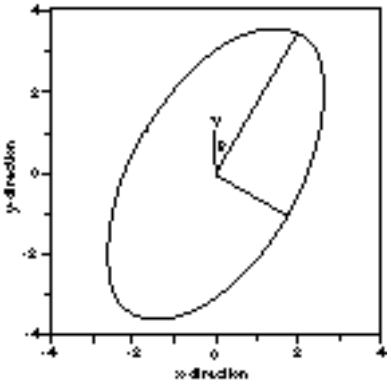

Figure 4. Example of geometric anisotropy, i.e. anisotropy in the range of the variograms. The longest axis (trending approximately Southwest–Northeast) is called the major axis. The axis perpendicular to this axis is called the minor axis. Source: PEBESMA (1999).

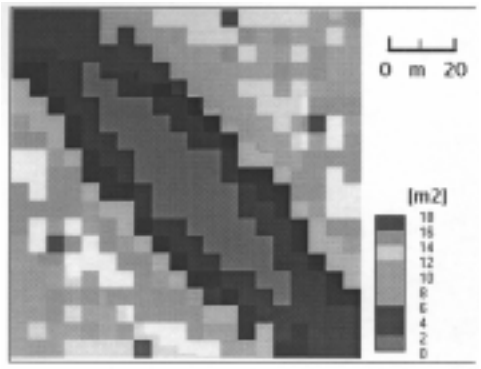

Figure 5. 2D representation of the variogram surface. The nugget is in the centre of the map, the semivariance increases to the outer rims of the map.

from North. This is an example of geometric anisotropy, because the sill that the minor axis reaches is later reached in the direction of the major axis. When this fact is incorporated in the interpolation action, the kriging results are expected to be more reliable than without this anisotropy.

Step 4: fitting of a variogram model

In this step, a graph of the semivariance is drawn and a variogram model is fitted by adjusting the fitting parameters by hand or automatically through one of the several methods of possible in Gstat. In this case, the first fitting was done by Gstat using 'weighted least squares' (WLS), the later 'fine tuning' was done manually. This optimising of the fit had to be done manually, because Gstat delivered variogram models with negative nuggets. These are known to be inadmissible (ISAAKS & SRIVASTAVA 1989; ARMSTRONG 1998). These nuggets were raised up to little above zero, in order to assure the soundness of the variogram model. To correct for the larger nugget, the sill was lowered with the same amount.

In almost all cases, variogram models that fit topographical data (i.e., height) are of the Gaussian type (BURROUGH, *pers. comm.*; PAZ GONZÁLEZ, *pers. comm.*; CACHEIRO POSE & VALCÁRCEL ARMESTO 1999). Also in this case, only Gaussian variogram models were fitted. This is because topography a very smoothly changing surface and this characteristic is reflected in the Gaussian model.

In figure 6, the three *isotropic* variograms with their fitted models are shown. It can be seen that the two variograms for the second and third order trend surface have a decrease in semivariance after the sill is reached, i.e. at distances longer than the range. This was the main reason for the choice of the first order trend surface to underlay the interpolation of the data set: its semivariogram can also be fitted adequately after the range with a single model. When the variogram decreases after the sill, this can be fitted by implementing an additional periodic variogram model (incorporating a sine function) but this model is hard to fit and results in an interpolation more prone to floating point and other errors.

The variogram of the first order trend surface however has an increase after the sill, indicating that the trend is not completely removed yet. Still, the variogram for the first order surface was chosen because of its better fit and longer range

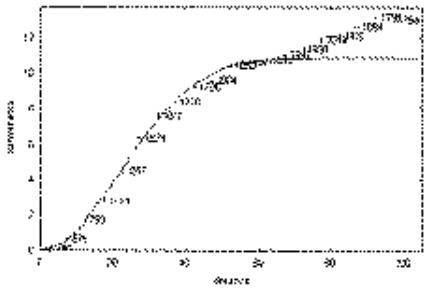

Figure 6a. The isotropic semivariogram after the application of the first order trend surface.

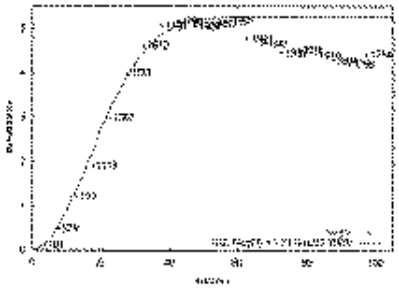

Figure 6b. The isotropic semivariogram after the application of the second order trend surface.

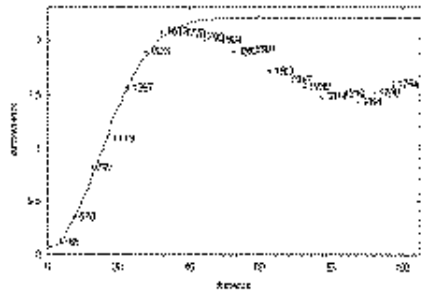

Figure 6c. The isotropic semivariogram after the application of the third order trend surface.

Figure 6. The three different isotropic variograms after implementation of a trend surface. Note the non-fit of the variograms after the range and the increase and decreases, respectively. Note also that the decrease of residuals with the increase in order is reflected in the semivariance values on the y axis [m^2].

than the second order trend surface variogram. The higher the sill and the longer the range of a variogram, the more structured it is and the better the interpolation results are (ARMSTRONG 1998).

Note that the above depicted variograms are only for illustration purposes, for they are all isotropic and an anisotropic variogram was used during kriging. In the subsequent variogram fitting, the anisotropy that was detected in Step 3 was implemented. This was done by adjusting in Gstat the search radius to a confined region, that has the same trend as either the major or the minor axis (see figure 7). The two variograms that emerge were evaluated to obtain the anisotropy ratio. In this case, this ratio is 0.5, i.e. the range in the direction of the major is half of that in the direction of the minor axis (geometric anisotropy).

The two anisotropic variograms for the residuals that are left after the application of the first order trend surface are shown in figure 8, one for the major axis and one for the minor axis. The fit for the variogram in the direction of the minor axis is not as good as that for the major axis, but still acceptable. Note that the sills are almost the same, about 12.3 m^2.

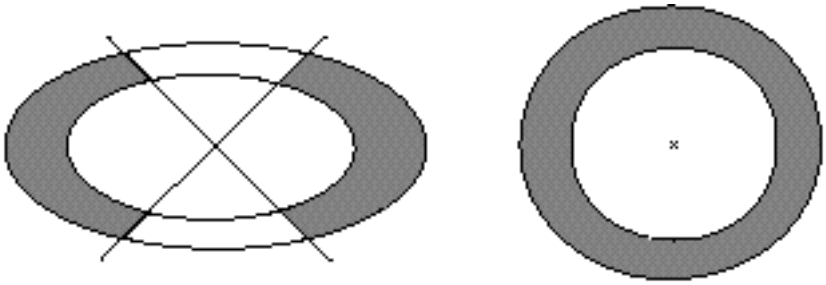

Figure 7. In the left figure, only the data that are located around the East–West trending major axis are used and subsequently only the data in the North–South direction are used for the calculation of the semivariogram in the direction of the minor axis (in the case of geometric anisotropy). In the right figure, the search radius that is normally used for isotropic variogram calculation is shown.

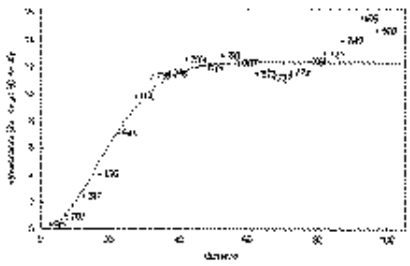

Figure 8a. The semivariogram in the direction of the minor axis (50º clockwise from North).

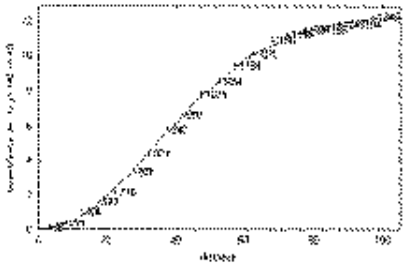

Figure 8b. The semivariogram in the direction of the major axis (140º clockwise from North).

Step 5: cross validation

In cross validation (also called x validation or jack-knifing), normally a comparison between different models (spherical, Gaussian, exponential etc.) that could be fitted through a data set is made. In this comparison, the model with the best statistics is used in the final interpolation. Here, the cross validation was used to choose between either anisotropic or isotropic variogram and between different radii for interpolation.

Cross validation proceeds through the interpolation on points were already a data point is available. The data value that is measured on the interpolated point is left out of the interpolation routine. This is done for all points and the measured and predicted results are compared. This comparison results in a correlation coefficient, which lies between 0 and 1; 0 denotes no

correlation at all between measured and predicted values, 1 denotes perfect correlation. Gstat calculates the Z score and the standard deviation as well. The Z score is calculated as the observed minus predicted value divided by the kriging standard deviation and should be as close to zero as possible. The standardised kriging standard deviation should be as close to one as possible.

In table 2, the results of the cross validation exercises are summarised. It was chosen to check for four different radii, i.e. 20, 30 and 40 m and a special radius optimised for the anisotropic variogram. This special radius is longer in the direction of the major axis and shorter in the direction of the minor axis (see also figure 7).

The r and Z statistics are satisfactory: both are close to one and zero, respectively. The standardised standard deviation σ^e, however, is far higher than one. The small kriging standard deviations are the explanation for this phenomenon. The (predicted minus observed) values are divided by these standard deviations. This causes the extremes of the Z distribution to be far away from zero (although the median and mean remain close to zero) and its standard deviation σ^e to be high. Because the lowest σ^e is reached by the special search radius of the anisotropic case, the interpolation was carried out using this special search radius. The σ^e value for this case is however still too high, but because the other two parameters indicate a well validated model and the parameter σ^e is rather sensitive, the model was still considered validated.

Step 6: final interpolation

The final interpolation was carried out with the above mentioned 'flexible' search radius and the prerequisite that at least 20 points were used in the interpolation. When this amount of data point could not be found within the search radius, Gstat was commanded to look for points outside the radius until the amount of 20 data points was reached.

The results are depicted in figure 9a, while the kriging standard deviations per pixel are depicted in figure 9b. Note that the borders exhibit high interpolation errors. This is due to a somewhat larger area of interpolation than the catchment in reality covers and a low amount of data points along the catchment borders. The delineation of the catchment borders follows later.

Of the 26,225 m^2 that is covered by

Statistic	i, 20 *	a, 20 *	i, 30	a, 30	i, 40	a, 40	a, 12 **
r	0.999	0.999	0.999	0.999	0.999	0.999	0.999
Z	−0.037	0.0016	0.0028	0.028	−0.015	−0.0024	−0.023
σ^e	2.36	2.28	2.82	2.36	3.02	2.78	2.17

Table 2. Cross validation results for isotropic and anisotropic variograms, for different interpolation radii. *): i denotes isotropic variogram and a denotes anisotropic variogram; **) 12 is the 'semivariance distance' in m^2.

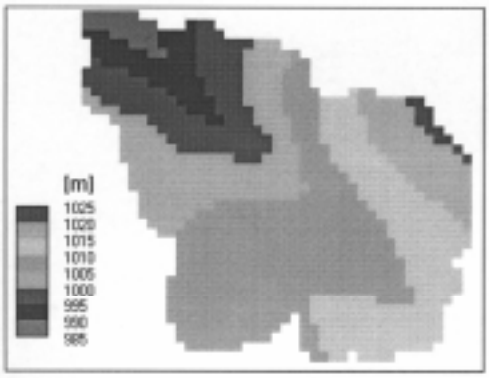

Figure 9a. The results of the interpolation, the digital elevation model (DEM) of the catchment.

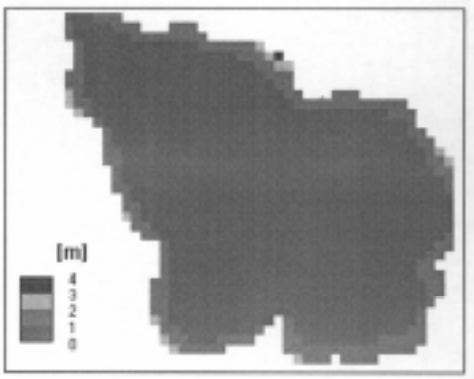

Figure 9b. The kriging standard deviations after the interpolation.

the interpolation, 21,500 m^2 has an interpolation error between three quarter of a meter and one meter. This sounds reasonable, but in a low-relief landscape like this catchment, this can have large influences on notably the runoff direction.

Furthermore, kriging is an interpolation method that generates a 'smoothed' interpolation surface, without the natural discontinuities or abrupt changes that in reality may be present in the landscape. An alternative method such as Monte Carlo simulation simulates a more natural 'rough' surface on basis of a given variogram and the (estimated) population standard deviation.

However, if the results are compared with another method of DEM creation, like digitising and rasterisation of analogue maps and remote sensing techniques, then it emerges that this method is relatively precise and determinate. Besides, the errors are known and this is not the case in several other methods of DEM elaboration. The knowledge of these errors helps in the evaluation of the outcomes of models that use the derivatives of DEM's.

CONCLUSIONS

Of the above discussion and presentation of the results, the following may be concluded:

· An interpolation with an anisotropic Gaussian variogram with the search radius adjusted to the anisotropy, applying Universal kriging with a first order trend surface, was the best kriging action possible in this case study.

· The quality of the interpolation is rather satisfactory when compared to other methods of DEM creation, but interpolation errors still may influence the derivatives of the DEM and so the subsequent outcome of the models that use these derivatives.

REFERENCES

ARMSTRONG, M. (1998). *Basic linear geostatistics*. Springer Verlag, Berlin (Germany). 153 pp.

BURROUGH, P.A. & McDONNELL, R.A. (1998). *Principles of Geographical Information Systems; Spatial information systems and geostatis - tics*. Oxford University Press. Oxford. UK. 333 pp.

CACHEIRO POSE, M. & VALCÁRCEL ARMESTO, M. (1999). Dependencia espacial de datos topográficos: interés para la elaboración de modelos de elevación digital. In: Paz González, A. & Taboada Castro, Ma. T. (eds.): *Avances sobre el estudio de la erosión hídrica*. Publicaciones UDC. Colección Cursos, Congresos, Simposios, nº 52, pp.: 59–60.

CACHEIRO POSE, M.; VALCÁRCEL M. & PAZ GONZÁLEZ, A. (1999). Medida automática de caudal y sedimentos en una pequeña cuenca experimental de Mabegondo. In: Paz González, A. & Taboada Castro, Ma. T. (eds.): *Avances sobre el estudio de la erosión hídrica*. Publicaciones UDC. Colección Cursos, Congresos, Simposios, nº 52, pp.: 239–260.

DAFONTE DAFONTE, J.; GONZÁLEZ GARCÍA, M. A.; PAZ GONZÁLEZ, A. & TABOADA CASTRO, Ma. T. (1999). Modelos digitales del terreno de dos cuencas agrícolas. In: Paz González, A. & Taboada Castro, Ma. T. (eds.): *Avances sobre el estudio de la erosión hídrica*. Publicaciones UDC. Colección Cursos, Congresos, Simposios, nº 52, pp.: 261–268.

ISAAKS, E. H. & SRIVASTAVA, R. M. (1989). *An introduction to applied geostatistics*. Oxford University Press, New York (USA), 561 pp.

KARSSENBERG, D. (1996). *PCRaster version 2 manual*. Department of Physical Geography, Faculty of Geographical Sciences, Utrecht University. Utrecht (The Netherlands), 368 pp.

KRIGE, D. G. (1966). Two-dimensional weighted moving average trend surface for ore –evaluation. *Journal of the South African Institute of Mining Metallurgy*, 66: 13–38.

PEBESMA, E. J. & WESSELING, C. G. (1998). Gstat: a program for geostatistical modelling, prediction and simulation. *Computers & Geosciences*, **24** (1):17–31.

PEBESMA, E.J. (1999). *gstat user's manual*. Department of Physical Geography, Faculty of Geographical Sciences, Utrecht University, Utrecht (The Netherlands), 100 pp. Also: http://www.geog.uu.nl/gstat/gstat.pdf.

Van DEURSEN, W.P. & WESSELING, C.G. (1992). *The PCRaster package*. Department of Physical Geography, Faculty of Geographical Sciences, Utrecht University, Utrecht (The Netherlands), 192 pp.